Organic & Biomolecular Chemistry

RSC Publishing

PAPER

View Article Online
View Journal | View Issue

Peptide–LNA oligonucleotide conjugates†

Cite this: *Org. Biomol. Chem.*, 2013, **11**, 4240

I. Kira Astakhova,*[a] Lykke Haastrup Hansen,[b] Birte Vester[b] and Jesper Wengel[a]

Although peptide–oligonucleotide conjugates (POCs) are well-known for nucleic acids delivery and therapy, reports on internal attachment of peptides to oligonucleotides are limited in number. To develop a convenient route for preparation of internally labeled POCs with improved biomedical properties, peptides were introduced into oligonucleotides *via* a 2′-alkyne-2′-amino-LNA scaffold. Derivatives of methionine- and leucine-enkephalins were chosen as model peptides of mixed amino acid content, which were singly and doubly incorporated into LNA/DNA strands using highly efficient copper(I)-catalyzed azide–alkyne cycloaddition (CuAAC) "click" chemistry. DNA/RNA target binding affinity and selectivity of the resulting POCs were improved in comparison to LNA/DNA mixmers and unmodified DNA controls. This clearly demonstrates that internal attachment of peptides to oligonucleotides can significantly improve biomolecular recognition by synthetic nucleic acid analogues. Circular dichroism (CD) measurements showed no distortion of the duplex structure by the incorporated peptide chains while studies in human serum indicated superior stability of the POCs compared to LNA/DNA mixmers and unmodified DNA references. Molecular modeling suggests strong interactions between positively charged regions of the peptides and the negative oligonucleotide backbones which leads to clamping of the peptides in a fixed orientation along the duplexes.

Received 25th March 2013,
Accepted 23rd April 2013

DOI: 10.1039/c3ob40786a

www.rsc.org/obc

Introduction

Interactions between nucleic acids and proteins are vital for important biological processes including, for example, storage and controlled processing of genetic information,[1,2] translation,[3] degradation of foreign polynucleotides by cellular restriction systems[4] and apoptosis.[5] Recently obtained crystal structures of natural nuclear DNA of eukaryotic cells and histone peptides[6] demonstrate the high importance of precise recognition between the biomolecules (Fig. 1). Furthermore, clinically important nucleic acid-based aptamers also utilize complex biomolecular recognition mechanisms when targeting proteins.[7–9]

Synthetic peptide–oligonucleotide conjugates (POCs) are artificial tools of choice for detailed studies of the abovementioned protein– and peptide–nucleic acid interactions, as well as being promising bioconjugates for nucleic acid delivery and therapy.[10] Two main strategies are currently available to prepare synthetic POCs.[10,11] The first is internal incorporation of a peptide residue *via* a chemically modified nucleotide scaffold of choice,[12,13] and the second is attachment of a peptide at terminal positions of an oligonucleotide (Fig. 1).[10,11,14,15] Internal labelling promotes active interaction between peptide and oligonucleotide chains, especially when they contain internally attached cationic peptides. Thereby the peptides have a high propensity for interacting with the nucleobases and the anionic backbones of oligonucleotides, and hence, to improve target binding and enzymatic stability of the POCs.[16–18]

Among various DNA linking strategies developed to date, the copper(I)-catalyzed azide–alkyne cycloaddition (CuAAC; or

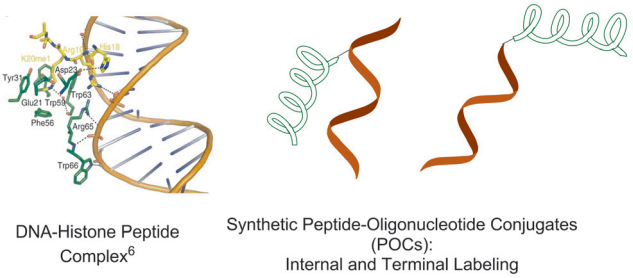

Fig. 1 Crystal structure of the histone peptide–nuclear DNA complex; schematic illustration of peptide–oligonucleotide conjugates (internal and terminal attachment).

[a]*Nucleic Acid Center and the Biomolecular Nanoscale Engineering Center, Department of Physics, Chemistry and Pharmacy, University of Southern Denmark, Campusvej 55, DK-5230 Odense M, Denmark. E-mail: ias@sdu.dk; Fax: +45 6615 8780; Tel: +45 6550 2523*

[b]*Department of Biochemistry and Molecular Biology, University of Southern Denmark, Campusvej 55, DK-5230 Odense M, Denmark. E-mail: b.vester@bmb.sdu.dk; Fax: +45 6550 2467; Tel: +45 6550 2406*

†Electronic supplementary information (ESI) available: Characterization of oligonucleotide conjugates, representative melting curves, CD spectra, autoradiograms of oligonucleotides incubated with HS, and molecular model of **POC2** : DNA are included in the ESI. See DOI: 10.1039/c3ob40786a

"click") reaction is one of the most selective and versatile.[19–21] As recently optimized by Finn *et al.*, the CuAAC reaction allows preparation of various oligonucleotide conjugates in high yields and of remarkable purity.[22–24] CuAAC click chemistry has been applied for preparation of several synthetic POCs.[14,25] This was carried out using azido-functionalized derivatives of membrane penetrating and nuclear localization signalling peptides.[14] Alternatively, azido-modified PNA and alkyne-modified amino acids were conjugated by the CuAAC reaction.[25] In both cases the desired POCs were obtained in high purity and yields.[14,25]

Locked nucleic acids (LNA) display excellent biomedical properties such as improved target binding affinity and enzymatic stability.[26–29] Moreover, incorporation of LNA has recently been shown to improve the therapeutic potential of oligonucleotides in siRNA and aptamer approaches.[30,31] Internal attachment of cationic amino acids to the 2′-amino group of 2′-amino-LNA by peptide coupling reactions resulted in increased binding affinity of the conjugates to complementary DNA/RNA targets.[32] Notably, the observed increase in thermal denaturation (T_m) values of the resulting conjugates was proportional to the total positive charge of the attached lysine residues. This was thought to be caused, at least in part, by decreased electrostatic repulsion between the negatively charged phosphate backbones and positively charged amino acid residues.[32]

Herein, we describe novel POCs in which peptide chains are internally incorporated into oligonucleotides using a 2′-alkyne-2′-amino-LNA scaffold (Fig. 2). The attachment of the selected methionine- and leucine-enkephalin peptides (Met- and Leu-enkephalins, respectively)[33] to 21-mer LNA/DNA mixmer strands was performed using highly efficient so-called postsynthetic CuAAC click chemistry (performed after the oligonucleotide is synthesized). There are several advantages to this design. First, internally attached enkephalin peptides having lysine extensions at the N-termini have high potential to interact with oligonucleotide strands.[16–18,32] Second, using highly efficient click chemistry, peptide chains can be incorporated into any position of oligonucleotide strands. Hence, the distance and orientation of the peptide residues could be estimated from well-known nucleic acid structure parameters. Third, a great diversity of other peptides, such as cell-penetrating[34] and for targeting of specific cells,[35] can be covalently tethered to the 2′-alkyne-2′-amino-LNA, opening up for various applications of this scaffold.

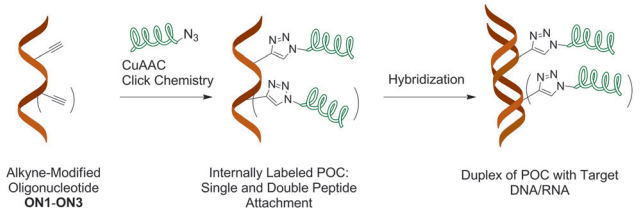

Fig. 2 General concept of CuAAC preparation of peptide–oligonucleotide conjugates (POCs) applied in this work.

In this paper we report the influence of internally attached enkephalin peptides on the structure and properties of synthetic oligonucleotides. We have prepared and studied single and double insertions of the peptides into LNA/DNA strands. We demonstrate that our novel synthesis strategy is rapid and efficiently provides series of POCs in high yields. Moreover, this approach allows us for the first time to evaluate target binding affinity, selectivity and enzymatic stability in human serum of an oligonucleotide containing covalently attached lysine-enkephalin hybrid peptides at internal positions.

Results and discussion

Strategy and design of enkephalin peptides "clicked" to LNA/DNA oligonucleotides

The general concept of POCs of this study is shown in Fig. 2. First, we synthesized 21-mer oligonucleotides containing single and double internal insertions of 2′-alkyne-LNA[36] monomer **M**^{1}. Similar **M**^{1}-labelled oligonucleotides were already applied for preparation and studies of fluorescent LNA/DNA probes (**ON1–ON3**, Table 1).[36,37] By combining the bicyclic LNA skeleton and a 2′-alkyne group, the monomer **M**^{1} is a very promising scaffold for preparation of POCs, providing a possibility of post-synthetic click chemistry along with precise positioning of the attached modifications within nucleic acid complexes.[37] Next, **ON1–ON3** were modified with enkephalin peptides by CuAAC conjugation with two azide-functionalized peptide derivatives **3–4** (Scheme 1). The number of nucleotides between two peptide modifications affects the distance, orientation and interactions between the peptides and the oligonucleotide scaffolds. Therefore we varied the number of nucleotides between the peptide residues by double insertion of monomers **M**^{1}–**M**^{3} (Table 1). Peptides of choice were short Met- and Leu-enkephalin derivatives containing three additional lysine residues at the N-termini (Scheme 1). The resulting peptides are amphiphilic and therefore display high solubility in both organic and polar aqueous media. This is of importance for efficient CuAAC reactions with oligonucleotides usually performed in mixtures of organic solvents and aqueous buffers, as well as for the purification of the products. Furthermore, Met- and Leu-enkephalins are targets of clinically important opioid receptors involved in pain and pleasure signalling.[38,39] Therefore the selected peptides can be potentially used as ligands for cell-specific delivery of oligonucleotides.

Post-synthetic CuAAC click chemistry for the preparation of POCs

Phosphoramidite **1** was prepared by following the recently described method[37] and was used in solid-phase oligonucleotide synthesis of conjugates **ON1–ON3** (characterized by MALDI-MS spectra and IE HPLC profiles) (Table 1, ESI Tables S1–S2, Fig. S1–S2†). Next, post-synthetic click chemistry of **ON1–ON3** with peptido-azide derivatives **3–4**, obtained from commercial suppliers, was performed. DMSO, 0.2 M carbonate

Table 1 Thermal denaturation temperatures (T_m values) of duplexes prepared in this study[a]

		$T_m/\Delta T_m$/°C			
		$[Na^+]$ = 110 mM		$[Na^+]$ = 20 mM	
		Duplex with complementary			
ON#	Sequence, 5′ → 3′	DNA	RNA	DNA	RNA
DNA^{ref}	TGC ACT CTA TGT CTG TAT CAT	59.0	60.5	39.0	43.0
ON1	TGC ACT CTA TG**M^1** CTG TAT CAT	62.0/+3.0	65.0/+4.5	41.0/+2.0	46.0/+3.0
ON2	TGC ACT CTA **M^1**GT C**M^1**G TAT CAT	63.5/+4.5	69.0/+8.5	44.0/+5.0	51.5/+8.5
ON3	TGC AC**M^1** CTA TGT CTG TA**M^1** CAT	63.0/+4.0	68.0/+7.5	43.0/+4.0	50.0/+7.0
POC1	TGC ACT CTA TG**M^2** CTG TAT CAT	60.0/+1.0	63.5/+3.0	43.0/+4.0	47.0/+4.0
POC2	TGC ACT CTA **M^2**GT C**M^2**G TAT CAT	65.0/+6.0	69.0/+8.5	47.0/+8.0	52.0/+9.0
POC3	TGC AC**M^2** CTA TGT CTG TA**M^2** CAT	63.0/+4.0	70.0/+9.0	39.0/±0.0	42.0/−1.0
POC4	TGC ACT CTA TG**M^3** CTG TAT CAT	62.0/+2.0	64.5/+4.0	47.0/+8.0	46.0/+3.0
POC5	TGC ACT CTA **M^3**GT C**M^3**G TAT CAT	64.0/+5.0	68.5/+8.0	48.0/+9.0	52.0/+9.0
POC6	TGC AC**M^3** CTA TGT CTG TA**M^3** CAT	58.0/−1.0	67.0/+6.5	43.0/+4.0	50.0/+7.0

[a] Thermal denaturation temperatures T_m (°C) (change in T_m relative to corresponding reference duplex DNA : DNA/RNA, ΔT_m (°C)). T_m values measured as the maximum of the first derivatives of the melting curves (A_{260} *vs.* temperature) using 0.5 μM concentration of complementary strands. Reported T_m values are averages of at least two measurements with resulting T_m ± 0.5 °C. Medium and low salt phosphate buffers ($[Na^+]$ = 110 mM and 20 mM, respectively, 0.1 mM EDTA, pH 7.0).

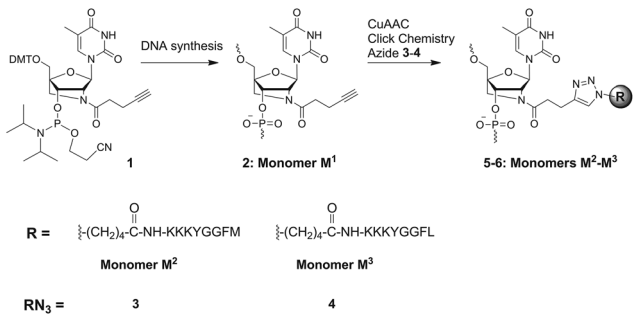

Scheme 1 Chemical structures of modified monomers **M^1–M^3**, phosphoramidite 1 and peptido-azides **3–4** used in this study. Sequences of natural enkephalins: YGGFM (Met-enkephalin); YGGFL (Leu-enkephalin).

buffer (pH 8.5), aminoguanidine hydrochloride, peptido-azide **3–4**,[40] $CuSO_4$–tri(benzyltriazolylmethyl)amine (TBTA)[41] (1 : 1) and sodium ascorbate were added to a deaerated aqueous solution of the starting oligonucleotide. The aminoguanidine hydrochloride was added in order to prevent aggregation and cross-linking of the peptide chains under the CuAAC conditions.[22,40] After 12–24 h at room temperature the product conjugates were purified on Sephadex (NAP-10) resin according to the protocol of the manufacturer followed by precipitation from cold acetone. The identity and purity of the POCs were confirmed by MALDI-MS spectra and IE HPLC profiles, respectively (Fig. S1–S2, ESI; Table S2†). The purity of POCs was ≥95% as estimated by IE HPLC, which was sufficient for their application in the studies described below without additional purification.

Yields of the products **POC1–POC6** were estimated using absorbance at 260 nm by a comparison of the amount of a POC product to the corresponding starting oligonucleotide and were 79%–88%. Notably, the yields were only slightly decreased for double incorporation of the peptide residues compared to single incorporation, and were similar for the double labelling in a 3 nucleotides and 11 nucleotides distance (ESI†).

Alternatively, the CuAAC reactions performed under microwave conditions in an argon atmosphere at 60 °C for 15 min resulted in similar yields of the POCs as following the procedure described above, although the purity of the products was lowered down to 87–93% (data not shown). This might be due to side reactions, *e.g.* cross-linking of the peptide residues, promoted by the microwave conditions and/or elevated temperature.

Hybridization properties and duplex structure

Strong and selective binding to complementary nucleic acids is a highly desired property for synthetic oligonucleotides which ensures their utility, *e.g.* for targeting of nucleic acids *in vitro* and *in vivo*.[42] Internally attached modifications, especially bulky and charged ones might significantly affect affinity of probes to targets.[42] In order to evaluate the effects of the novel monomers **M^2** and **M^3** on the hybridization properties of LNA/DNA oligonucleotides, we determined thermal denaturation temperatures (T_m) of the duplexes formed by **POC1–POC6** with complementary DNA/RNA, and we compared the resulting T_m values to those of the unmodified (**DNA^{ref}**) and corresponding **M^1**-functionalized duplexes (Table 1). The thermal denaturation experiments were performed in medium and low salt phosphate buffers ($[Na^+]$ = 110 mM and 20 mM, respectively, 0.1 mM EDTA, pH 7.0) using 0.5 μM concentration of the two complementary strands (Table 1). All the T_m curves recorded for modified oligonucleotides displayed S-shaped monophasic transitions similar to those of the unmodified reference duplexes (Fig. S3, ESI†). Generally duplexes of the prepared POCs displayed higher T_m values when bound to the RNA target than to the DNA target. This is in good agreement with

Table 2 Effect of single-nucleotide mismatch on binding affinity of **POC3** and **POC5** to DNA/RNA targets in a medium salt buffer[a]

		T_m/°C							
		DNA target				RNA target			
POC: target duplex[a]	X=	A	C	T	G	A	C	U	G
5′-TGC ACT CTA **M²**GT C**M²**G TAT CAT 3′-ACG TGA GAT ACA GAXATA GTA		54.0	65.0[cc]	58.0	55.0	50.0	69.0[cc]	52.0	58.0
5′-TGC ACT CTA **M²**GT C**M²**G TAT CAT 3′-ACG TGA GAT ACA GXC ATA GTA		65.0[cc]	57.0	58.0	55.0	69.0[cc]	53.5	61.0	55.0
5′-TGC ACT CTA **M²**GT C**M²**G TAT CAT 3′-ACG TGA GAT XCA GAC ATA GTA		65.0[cc]	55.0	57.0	57.0	69.0[cc]	61.0	60.5	63.5
5′-TGC ACT CTA **M²**GT C**M²**G TAT CAT 3′-ACG TGA GAXACA GAC ATA GTA		57.0	56.0	65.0[cc]	52.0	61.0	69.0[cc]	61.0	63.0
5′-TGC AC**M²** CTA TGT CTG TA**M²** CAT 3′-ACG TGA GAT ACA GAC ATA XTA		53.0	56.0	53.0	63.0[cc]	50.0	50.0	49.0	70.0[cc]
5′-TGC AC**M²** CTA TGT CTG TA**M²** CAT 3′-ACG TGA GAT ACA GAC ATXGTA		63.0[cc]	52.0	55.0	53.0	70.0[cc]	52.0	50.0	49.0
5′-TGC AC**M²** CTA TGT CTG TA**M²** CAT 3′-ACG TGA GAT ACXGAC ATA GTA		63.0[cc]	54.0	54.0	55.0	70.0[cc]	55.0	48.0	50.0
5′-TGC AC**M²** CTA TGT CTG TA**M²** CAT 3′-ACG TGA XAT ACA GAC ATA GTA		49.0	51.0	48.0	63.0[cc]	n.t.	48.0	49.0	70.0[cc]

[a] Sequences of DNA target variants are displayed; cc = complementary complex; n.t. = no clear transition detected. Medium salt phosphate buffer ([Na^+] = 110 mM, 0.1 mM EDTA, pH 7.0). T_m values measured using 0.5 μM concentration of complementary strands.

previous data on stability of nucleic acid complexes containing derivatives of 2′-amino-LNA.[27,29] Single insertion of monomer **M²** and **M³** did not affect T_m values of the resulting duplexes compared to insertion of **M¹** but improved binding affinities (ΔT_m + 2–4 °C) were observed relative to the unmodified reference duplexes. In the case of double modification, conjugates containing monomers **M²** or **M³** spaced by 3 nucleotides showed generally higher T_m values than conjugates having an 11 nucleotide distance between the attached peptides. This implies a stabilizing interaction between the attached moieties arising in the former complexes (Table 1, data for **POC2** and **POC5** compared to **POC3** and **POC6**, respectively). The superior duplex stability obtained with the double-labeled POCs relative to unmodified and **M¹**-containing references could furthermore result from the increased flexibility of the former probes, which might be beneficial for a more favourable entropy term for complex formation.[43]

The T_m values of duplexes formed by the POCs were strongly decreased in a low salt medium although a significant stabilizing effect was observed when comparing the POCs with the unmodified references under similar conditions. It is noteworthy that proximate and distant incorporation of peptides resulted in much higher difference of T_m values measured in the low salt buffer than in the medium salt buffer. This was especially significant for **M²**-labeled **POC2** and **POC3** which displayed up to 10 °C higher T_m values with a 3 nucleotide linker than with an 11 nucleotide linker. Altogether, the observed stabilization of the duplexes formed by POCs in both medium and low salt media suggests successful orientation of the attached peptides along the double-stranded nucleic acid complexes.

Next, we investigated the sensitivity of the selected POCs and corresponding **M¹**-labeled precursors toward single-nucleotide mismatches at different sites along the target DNA/RNA (Table 2 and Tables S3–S4, ESI†). Single incorporation of monomer **M²** or **M³** resulted in a decrease in T_m values in the presence of a single-nucleotide mismatch in all the investigated positions along the target DNA/RNA. The decrease in binding affinity was of similar magnitude for **POC1**, **POC4** and the LNA reference **ON1** ($\Delta T_m \sim 12$ °C and ~14 °C for DNA and RNA targets, respectively, in comparison to fully complementary complexes; Table S3, ESI†). In contrast, double insertion of the peptides resulted in superior mismatch sensitivity of the POCs relative to **M¹**-labeled oligonucleotides (Table 2 compared to Table S4, ESI†).

Generally, a mismatch opposite to **M²** within **POC2** and **POC3** was discriminated in a similar manner as if being located 1 nucleotide next to the modification. This is opposed to the typical behaviour of LNA/DNA conjugates, usually displaying better discrimination of a mismatch located opposite to an LNA nucleotide.[29] Among the double-labeled conjugates, **POC3** showed superior mismatch discrimination in binding both DNA and RNA targets (Table 2). The T_m decrease for **POC3** in the presence of a single-nucleotide mismatch was 8–13 °C and 5–10 °C for DNA and RNA targets, respectively, when compared to **M¹**-labeled reference **ON3**. It is noteworthy that T_m values for all the POCs investigated were less dependent on the type of mismatched nucleotide when compared to

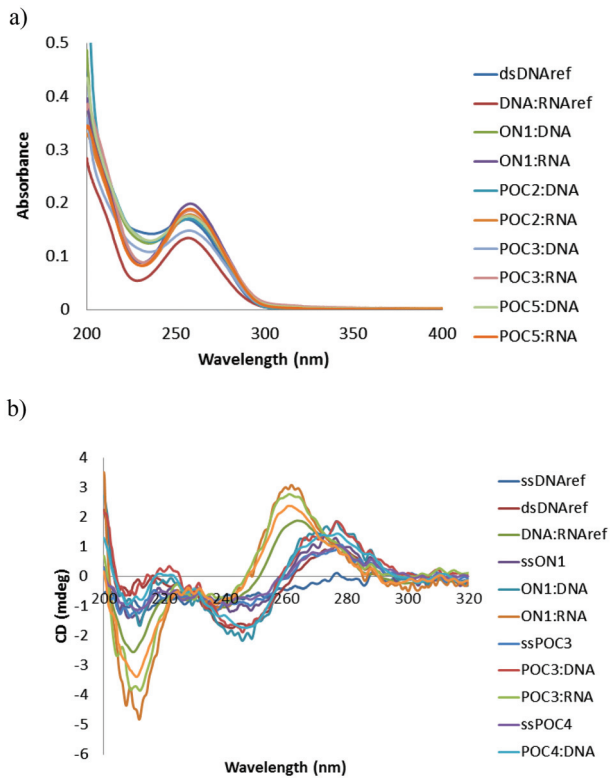

Fig. 3 Representative UV-Vis (a) and CD spectra (b) of POCs and reference oligonucleotides/duplexes. The spectra were recorded in a medium salt buffer at 19 °C using 2.0 μM concentration of complementary strands.

the references **ON1–ON3**. The observed sensitivity of the double-labeled POCs to single-nucleotide mismatches points to the strong impact of the attached peptides on the probes' binding properties.[42] Importantly, a low sensitivity of the prepared POCs to the nature of mismatched nucleobase and its position along the target strand exclude the possibility of intercalation or placing of the attached peptide moieties within the groove of the duplexes, since both these modes involve active interaction between the modification and the nucleic acid complex.[29]

To investigate the structure of the duplexes we measured UV-Vis and CD spectra. As can be seen from Fig. 3, all the duplexes involving the POCs displayed exclusively characteristic oligonucleotide absorption bands in the UV region at λ^{max} ~ 259–262 nm. Next, CD curves indicated intermediate A/B duplex geometry of the duplexes similar to the control LNA/DNA duplexes.[44] Compared to the unmodified reference duplexes, LNA-induced perturbation of duplex geometry resulted in simultaneously shifted CD maxima and changed peak intensities. Thus, A/B-type duplexes formed by the POCs prepared herein displayed strong CD signals around 210 nm and 260 nm of negative and positive magnitude, respectively, accompanied by a week negative signal at ~240 nm (Fig. 3b). However, having very low molar extinction coefficients ε ~ 200–1500 cm^{-1} M^{-1}, the attached peptides did not provide any additional signals in the UV-Vis or CD spectra. Furthermore, the similarity of CD curves observed for the POCs and reference LNA/DNA oligonucleotides excludes structural perturbation of the complexes by the modification with peptides, and we can assume that the attached peptides successfully allow the formation of a stable A/B-type duplex structure typical for LNA/DNA conjugates. Finally, no difference was observed between UV-Vis and CD spectra of POCs having monomers $\mathbf{M^2}$ and $\mathbf{M^3}$, most likely owing to the structural similarity of the Met- and Leu-enkephalins, and to the low optical impact of the peptides (Fig. S4, ESI†).

Stability of POCs in human serum

Stability of synthetic oligonucleotides in diverse biological media, including human serum (HS), is of crucial significance for their application as diagnostic and therapeutic tools *in vivo*.[45] Chemical modification with synthetic nucleotide analogues, especially LNA,[46] is known to dramatically improve the enzymatic stability of oligonucleotides.[42,46] In our study we investigated the stability of the novel POCs in a weakly diluted HS, a complex medium containing several classes of enzymes, which is very similar to the media of *in vivo* studies and clinical trials.[47] In these experiments, unmodified DNA reference and $\mathbf{M^1}$-labeled analogues were used as controls.

We chose **POC2** and **POC5** for the serum stability studies, since these conjugates displayed high target binding affinities and selectivity (Tables 1 and 2). The POCs of choice and the corresponding controls were 5′-end labeled with ^{32}P and incubated in HS according to the protocol in the ESI.† Samples were withdrawn after 2, 5, 10, 30 min and after 1, 4, 8, and 24 h and resolved on denaturing (7 M urea) acrylamide gels

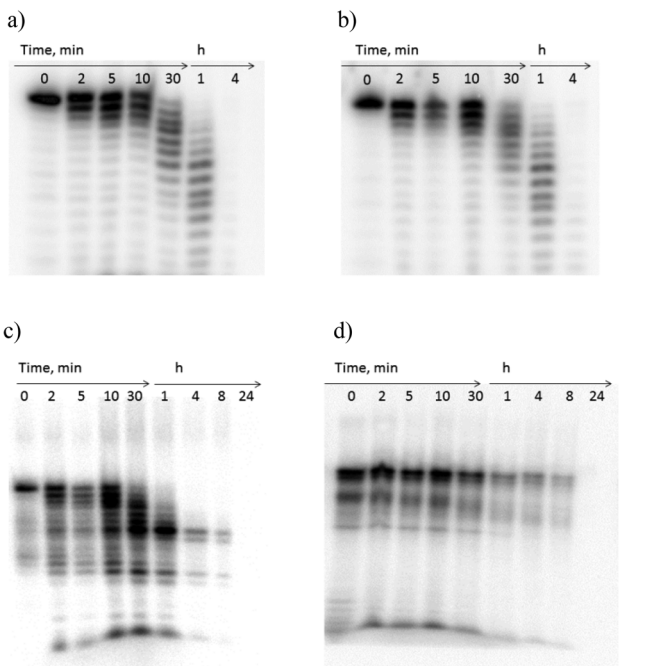

Fig. 4 Gel electrophoresis of 5′-^{32}P-labeled oligonucleotides after incubation in human serum; (a and b) unmodified reference DNA in 90% and 10% serum, respectively, (c) **ON2** (in 90%, serum), and (d) **POC2** (in 90% serum).

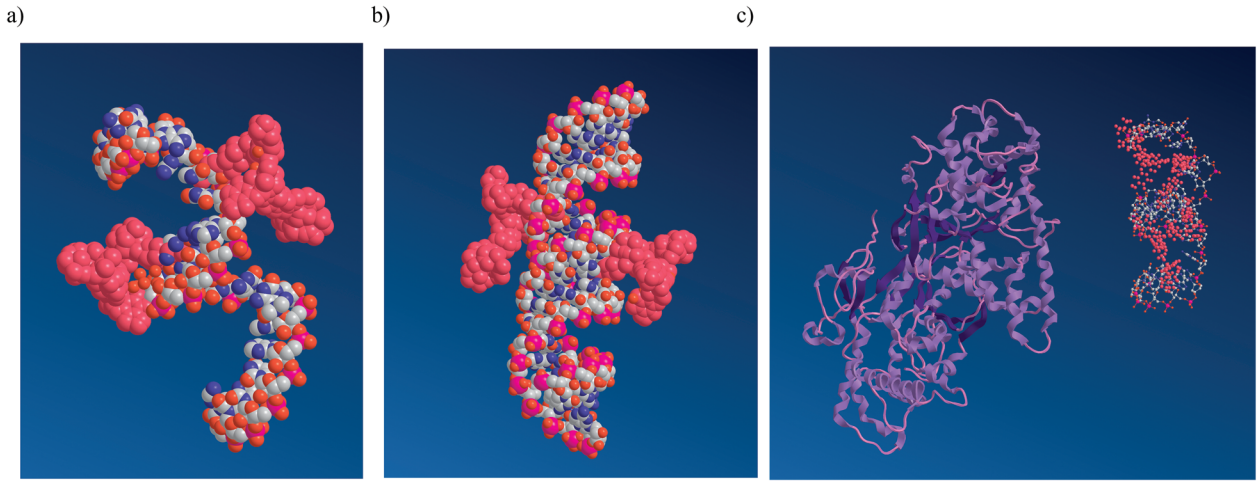

Fig. 5 Representative energy-minimized structures: (a) ss**POC5**, (b) **POC5** : DNA, and (c) ss**POC5** and human exonuclease 1 (no interaction due to shielding by the peptide residues). Nucleic acids are shown as white, red, pink and blue balls corresponding to carbon, oxygen, phosphorus and nitrogen atoms, respectively; hydrogen atoms are not shown; peptide residues are indicated in crimson; human exonuclease 1 is shown in purple (c).

(Fig. 4; Fig. S5, ESI†). As is evident from Fig. 4, the unmodified **DNA^{ref}** was degraded already within 30 min, even when HS was diluted to 10% (Fig. 4a and b). The LNA/DNA reference **ON2** was degraded within 1 h in a 90% HS (Fig. 4c). Interestingly, the partial products of degradation of **ON2** displayed substantial stability (>8 h, Fig. 4c). The autoradiogram observed for **ON2** points to stability of the LNA modified conjugates after cleavage close to modified position 14. In turn, the peptide-modified analogues **POC2** and **POC5** demonstrated significant resistance to enzymatic cleavage in 90% HS (>8 h; Fig. 4d and Fig. S5, ESI†). The two characteristic bands observed for both POCs could be referred to the heterogeneity of the prepared conjugates (purity ≥ 95% as evaluated by IE HPLC) or following radiolabelling, as two bands were observed in the initial samples (0 min). Finally, the complete disappearance of the bands after 8 h might be due to phosphatase activity of HS removing the ^{32}P-labels from the POCs.[47]

Notably, the resistance of the investigated **POC2** and **POC5** to degradation up to 8 h was comparable and even superior to previously reported stabilities of other modified oligonucleotides in complex biological media.[47] For example, J. Kurreck *et al.* investigated the stability of LNA/DNA antisense mixmers in diluted HS, which digested unmodified control 18-mer DNA in 3–4 h.[47] The authors observed stability up to 15 h for the LNA/DNA chimeras, when the probes had four sequential incorporations of LNA nucleotides at both the 3′- and 5′-termini. Notably, in a recent work by N. K. Andersen *et al.*, a dramatic degradation of internally-labeled oligonucleotides having phenyl-triazole modifications was reported within 15 min after treatment with diluted fetal calf serum.[47] The increased stability of the POCs prepared herein is due to the peptide residues attached to single-stranded oligonucleotides,[18] combined with the stabilization achieved due to the presence of the 2′-amino-LNA nucleotides.[47]

Additional digestion experiments with HS pre-treated with 1 mM diethyl 4-nitrophenyl phosphate (paraoxon-ethyl), selectively inhibiting the proteolytic activity of the serum, explained the mechanism of the observed digestion.[48] Thus, experiments with HS pre-treated with paraoxon-ethyl revealed similar degradation patterns for **POC2** and **POC5** as in the case of the initial assay, confirming the nuclease attack as a main digestion mechanism (Fig. S5c and d, ESI†).

Molecular modelling

To further rationalize the obtained experimental data, molecular models of the single-stranded POCs and their duplexes were built (Fig. 5 and Fig. S6, ESI†). The initial structures were built and modified with LNA monomers in the B-type duplex conformation using the MacroModel suite of programs.[49,50] Having minimized the structures using the AMBER force field as implemented by MacroModel,[51] the models were imported into the Chem3D Pro 12.0 program, where the peptide residues, created using ChemDraw Ultra 12.0, were attached to the 2′-amino-LNA scaffolds. The resulting structures were minimized and afterwards subjected to MM2 dynamics (ESI†).[52] The obtained complexes were further analyzed in Swiss-Pdb Viewer 4.1.0, where a structure of the dsDNA binding human exonuclease 1 was imported (Fig. 5c and ESI†).[53] Finally, graphical images were processed in the PyMOL Molecular Graphics System. Models of the resulting single-stranded POCs and duplexes, as well as of the lack of interaction with human exonuclease 1, are shown in Fig. 4. As one can see, modeling indicated successful positioning of the peptides along single-stranded oligonucleotides and duplexes (Fig. 5a and b). The modelling does not support intercalation and/or positioning of the attached residues within the grooves, as previously reported for 2′-amino-modified analogues of 2′-amino-LNA.[29] The minor influence of the attached peptide modifications on the duplex structure agrees with the observed low sensitivity of the POCs to a single-nucleotide mismatch in DNA/RNA targets (Table 2). Remarkably, but in good agreement with the CD spectra described above, we did not observe any difference in

duplex parameters between conjugates possessing monomers $\mathbf{M^2}$ and $\mathbf{M^3}$ (Fig. S6, ESI†). We can also conclude that a small variation at the C-termini of the peptide residue within monomers $\mathbf{M^2}$ and $\mathbf{M^3}$ has only a minor effect on the duplex geometries, hydration and electrostatic properties, resulting in similar melting temperatures and CD profiles of the duplexes, containing internally attached Met- and Leu-enkephalins.

Finally, an effective association of the peptide residues with single-stranded oligonucleotide chains was observed in the model of ss**POC5** (Fig. 5a). The proposed association is most likely caused by electrostatic interactions and hydrogen bonding between the peptide residues and nucleic acid phosphate backbone, as well as by hydrogen bonding between the peptides and nucleobases.[18] This type of structure is in good agreement with the high enzymatic stability of the POCs, as the internally attached peptides provide shielding of the oligonucleotide strand, which prevents interaction of the POCs with the enzymes present in HS, *e.g.* human exonuclease 1 (Fig. 5c).

Experimental methods

Reagents

Phosphoramidite **1** was prepared as described.[37] Peptide strands derivatized with terminal azide groups **3–4** and TBTA[41] for click chemistry were obtained from Caslo ApS, Denmark, and Lumiprobe LLC, respectively. Other reagents and solvents were used as received. Stock solutions for click chemistry were prepared as described.[23,24] Human serum (HS), paraoxon-ethyl and Hank's buffered salt solution (HBSS) were purchased from Sigma-Aldrich; enzymatic activity of the serum was confirmed by following a published protocol.[48]

Synthesis of oligonucleotides ON1–ON3

Oligonucleotide synthesis was carried out on a PerSpective Biosystems Expedite 8909 instrument in the 1 μmol scale using the manufacturer's standard protocols. For the incorporation of monomer $\mathbf{M^1}$ a hand-coupling procedure was applied (25 min coupling). The coupling efficiencies of standard DNA phosphoramidites and reagent **1** based on the absorbance of the dimethoxytrityl cation released after each coupling varied between 95% and 100%. Cleavage from a solid support and removal of nucleobase protecting groups were performed using 32% aq. ammonia and methylamine 1 : 1, v/v, for 4 h at rt. The resulting oligonucleotides were purified by DMT-ON RP-HPLC using the Waters System 600 equipped with an Xterra MS C18-column (5 μm, 150 mm × 7.8 mm). Elution was performed starting with an isocratic hold of A-buffer for 5 min followed by a linear gradient to 70% B-buffer over 40 min at a flow rate of 1.0 mL min^{-1} (A-buffer: 0.05 M triethyl ammonium acetate, pH 7.4; B-buffer: 25% buffer A, 75% CH_3CN). RP-purification was followed by detritylation (80% aq. AcOH, 30 min), precipitation (acetone, −18 °C, 12 h) and washing with acetone two times. The identity and purity of the oligonucleotides were then verified by MALDI-TOF mass spectrometry and IE HPLC, respectively (ESI†). MALDI-TOF mass-spectrometry analysis was performed using a MALDI-LIFT system on the Ultraflex II TOF/TOF instrument from Bruker and using a HPA-matrix (10 mg 3-hydroxypicolinic acid, 50 mM ammonium citrate in 70% aqueous acetonitrile). IE HPLC was performed using a Merck Hitachi LaChrom instrument equipped with a Dionex DNAPac Pa-100 column (250 mm × 4 mm). Elution was performed at 60 °C starting with an isocratic hold of A- and C-buffers for 2 min followed by a linear gradient to 60% B-buffer over 28 min at a flow rate of 1.0 mL min^{-1} (A-buffer: MQ water; B-buffer: 1 M $NaClO_4$, C-buffer: 25 mM Tris-Cl, pH 8.0). Unmodified DNA/RNA strands were obtained from commercial suppliers and used without further purification.

Post-synthetic click chemistry

Concentrations of oligonucleotides were calculated using the following extinction coefficients (OD_{260}/μmol): G, 10.5; A, 13.9; T, $\mathbf{M^1}$, 7.9; C, 6.6; $\mathbf{M^2}$, 8.1; $\mathbf{M^3}$, 9.2. Extinction coefficients at 260 nm of monomers $\mathbf{M^2}$–$\mathbf{M^3}$ were determined by summarizing the extinction coefficient of monomer $\mathbf{M^1}$ and the corresponding azide **3–4**. The latter values were measured at 19 °C in 5% DMSO–water, v/v.

General method for CuAAC reactions. Starting oligonucleotide **ON1–ON3** (20 nmol) was dissolved in fresh MQ water (30 μL) in a 1.5 mL plastic eppendorf. DMSO (40 μL), 0.2 M carbonate buffer (pH 8.5; 10 μL), corresponding azide **3–4** (6 μL (**ON1**) and 10 μL (**ON2–ON3**) of a 10 mM solution in 30% DMSO–0.02 M carbonate buffer), aminoguanidine hydrochloride (5 μL of a 50 mM freshly prepared stock solution), ascorbic acid (5 μL of a 25 mM freshly prepared stock solution) and the Cu(II)–TBTA equimolar complex (5 μL of a 10 mM stock solution) were subsequently added. The resulting mixture was deaerated using argon, tightly closed, mixed by vortexing and left at rt for 12 h (**ON1**) or 24 h (**ON2–ON3**). The reaction was afterwards filtrated through an Illustra NAP-10 column (GE Healthcare) following the manufacturer's protocol. The resulting solution was evaporated followed by precipitation of the product conjugates from cold acetone (−18 °C, 12 h) and subsequent washing with acetone two times. The resulting conjugates **POC1–POC6** were analyzed by MALDI-TOF mass spectrometry and IE HPLC as described above (Table S2, Fig. S1–S2, ESI†). Final yields of the products based on absorbance at 260 nm: 88% (**POC1**), 84% (**POC2**), 78% (**POC3**), 70% (**POC4**), 82% (**POC5**), 79% (**POC6**).

UV-visible absorbance and thermal denaturation studies

UV-visible absorbance spectra and thermal denaturation experiments were performed on a Beckman Coulter DU800 UV/VIS spectrophotometer equipped with a Beckman Coulter High Performance Temperature Controller in a medium salt phosphate buffer (100 mM NaCl, 2 mM NaH_2PO_4, 8 mM Na_2HPO_4, 0.1 mM EDTA, pH 7.0), and a low salt phosphate buffer (10 mM NaH_2PO_4, 10 mM Na_2HPO_4, 0.1 mM EDTA, pH 7.0). Concentrations of oligonucleotides and POCs were calculated using the extinction coefficients listed above. Complementary strands (0.5 μM of each strand) were thoroughly mixed, denaturated by heating for 10 min at 85 °C and subsequently

cooled to the starting temperature of the experiment (15 °C). Thermal denaturation temperatures (T_m values, °C) were determined as the maximum of the first derivative of the thermal denaturation curve (A_{260} *vs.* temperature). Reported T_m values are an average of at least two measurements with the resulting T_m within ±0.5 °C.

CD measurements

CD spectra were recorded on a JASCO J-815 CD spectrometer equipped with a CDF 4265/15 temperature controller. Samples for CD measurements were prepared as described in the UV-visible absorbance and thermal denaturation studies section except that a concentration of 2.0 μM of both strands was used. Quartz optical cells with a path-length of 0.5 cm were used.

Serum stability assay

The oligonucleotides were ^{32}P-labeled at the 5′-end with T4 kinase by following standard procedures. 0.1 pmol radioactive oligonucleotides mixed with 3.9 pmol unlabelled oligonucleotide were added to human serum (16 μL, 90% or 10% in HBSS buffer, pH = 7.4) in a pcr tube in a total volume of 20 μL. Pretreatment of the human serum with 1 mM solution of paraoxon-ethyl was performed as decribed.[48] The samples were incubated in an Eppendorf Mastercycler personal at 37 °C. The aliquots were withdrawn after 2 min, 5 min, 10 min, 30 min, and 1 h, 4 h, 8 h and 24 h time intervals and quenched with 1 vol of ice-cold 95% formamide with excess EDTA. The incubated samples were then resolved on 13% denaturing polyacrylamide gels (7 M urea; 1× TBE) and visualized by autoradiography on a Typhoon Trio Variable Mode Imager (Amersham Biosciences).

Molecular modelling

The initial oligonucleotides were built and modified with LNA monomers in the B-type duplex conformation in the MacroModel suite of programs.[49] The minimization was performed using the AMBER force field as implemented by MacroModel.[50] Peptide residues were incorporated into the resulting low-energy structures using ChemBioDraw Ultra 12.0 and Chem3D Pro 12.0. The structures were further minimized by MM2 as implemented in Chem3D Pro 12.0 and subjected to MM2 dynamics (step interval: 2; frame interval: 10; heating speed: 1 K; target temperature: 300 K).[51] Resulting structures were further analyzed using Swiss-Pdb Viewer 4.1.0. The structure of the human exonuclease 1 used in the modeling of interactions with **POC2** was adopted from Pdb databank and used without modification.[53] Resulting structures were additionally processed in the PyMOL Molecular Graphics System.

Conclusions

In summary, we have successfully developed a new strategy for internal CuAAC labeling of LNA/DNA oligonucleotides with peptides and applied it for the preparation of novel POCs possessing internal peptide groups. This method gives high yields and allows incorporation of peptides into desired positions of oligonucleotides *via* a chemically and enzymatically stable 1,2,3-triazole linker.[54] Our system using 2′-amino-LNA as a new scaffold for CuAAC attachment of peptides will be suitable for the incorporation of other groups (such as cell-penetrating peptides,[55] carbohydrates,[56] and small molecules[57]) into synthetic oligonucleotides. This can significantly benefit the preparation strategy of modified oligonucleotides as advanced tools for nanobiotechnology, supramolecular chemistry and chemical biology.

Moreover, attachment of peptides to 2′-amino-LNA by CuAAC chemistry allowed us for the first time to study in detail target binding affinity and selectivity, spectral behaviour and enzymatic stability of an oligonucleotide containing clinically and biologically important enkephalins in the internal positions. Of particular note is the hybrid nature of the prepared peptides, combining encephalin residues with cationic lysines, providing high propensity to interaction with nucleic acids. The performed studies indicated high affinity and selectivity of the prepared POCs to complementary DNA and RNA targets. POCs having double incorporation of peptides separated by three nucleotides showed up to 8 h stability in weakly diluted human serum (90%), whereas LNA/DNA and unmodified DNA controls were degraded in 1 h and 30 min, respectively. The experimental data of the POCs were in good agreement with molecular modeling. The oligonucleotide chain, which is typically rapidly degraded by complex enzyme composition of human serum, appears to be protected from digestion by shielding peptide chains located outside the helix. The results presented demonstrate that the properties of oligonucleotides can be strongly influenced by internally conjugated peptides. The novel internally labeled POCs described herein have a high potential for applications both *in vitro* and *in vivo*.

Acknowledgements

The Sapere Aude programme of the Danish Council for Independent Research is acknowledged for funding. The VILLUM FOUNDATION is thanked for funding the Biomolecular Nanoscale Engineering Center.

Notes and references

1 M. Parisien, K. F. Freed and T. R. Sosnick, *PLoS One*, 2012, **7**, e32647.
2 R. Sukackaite, S. Grazulis, G. Tamulaitis and V. Siksnys, *Nucleic Acids Res.*, 2012, **40**, 7552; M. AlQuraishi and H. H. McAdams, *Proc. Natl. Acad. Sci. U. S. A.*, 2011, **108**, 14819.
3 M. Cox and D. R. Nelson, *Lehninger principles of biochemistry*, 4th edn, W.H. Freeman, New York, 2005.

4 M. Simons and M. D. Szczelkun, *Nucleic Acids Res.*, 2011, **39**, 7656.
5 S. Abe, M. Kurata, S. Suzuki, K. Yamamoto, K. Aisaki, J. Kanno and M. Kitagawa, *PLoS One*, 2012, **7**, e40129.
6 D. Kim, B. J. Blus, V. Chandra, P. Huang, F. Rastinejad and S. Khorasanizadeh, *Nat. Struct. Mol. Biol.*, 2010, **17**, 1027.
7 H. Kaur and L.-Y. Lanry Yung, *PLoS One*, 2012, **7**, e31196.
8 V. G. B. Ruigrok, M. Levisson, J. Hekelaar, H. Smidt, B. W. Dijkstra and J. van der Oost, *Int. J. Mol. Sci.*, 2012, **13**, 10537.
9 L. Meng, L. Yang, X. Zhao, L. Zhang, H. Zhu, C. Liu and W. Tan, *PLoS One*, 2012, **7**, e33434.
10 B. A. R. Williams and J. C. Chaput, *Curr. Protoc. Nucleic Acid Chem.*, 2010, **42**, 4.41.1; D. A. Stetsenko and M. J. Gait, *Methods Mol. Biol.*, 2004, **288**, 205; V. Marchán, E. Pedroso and A. Grandas, *Chem.–Eur. J.*, 2004, **10**, 5369.
11 J. D. Carter and T. H. LaBean, *J. Nucleic Acids*, 2011, **2011**, 926595.
12 F. Diezmann, H. Eberhard and O. Seitz, *Biopolymers*, 2010, **94**, 397.
13 M. Frieden, A. Aviñó, G. Tarrasón, M. Escorihuela, J. Piulats and R. Eritja, *Chem. Biodiversity*, 2004, **1**, 930; D. Gottschling, H. Selinger, G. Tarrasón, J. Piulats and R. Eritja, *Bioconjugate Chem.*, 1998, **9**, 831.
14 M. Wenska, M. Alvira, P. Steunenberg, Å. Stenberg, M. Murtola and R. Strömberg, *Nucleic Acids Res.*, 2011, **39**, 9047.
15 T. P. Wang, N. C. Ko, Y. C. Su, E. C. Wang, S. Severance, C. C. Hwang, Y. T. Shih, M. H. Wu and Y. H. Chen, *Bioconjugate Chem.*, 2012, **23**, 2417.
16 W. Gong, T. Zhou, J. Mo, S. Perrett, J. Wang and Y. Feng, *J. Biol. Chem.*, 2012, **287**, 8531; A. E. Rapoport and E. N. Trifonov, *Gene*, 2011, **488**, 41.
17 C. M. Santiveri, B. C. Lechtenberg, M. D. Allen, A. Sathyamurthy, A. M. Jaulent, S. M. Freund and M. Bycroft, *J. Mol. Biol.*, 2008, **382**, 1107.
18 J. G. Harrison and S. Balasubramanian, *Nucleic Acids Res. Suppl.*, 1998, **26**, 3136, and references therein.
19 C. Spiteri and J. E. Moses, *Angew. Chem., Int. Ed.*, 2010, **49**, 31, and references therein.
20 C. W. Tornøe, C. Christensen and M. Meldal, *J. Org. Chem.*, 2002, **67**, 3057.
21 V. V. Rostovtsev, L. G. Green, V. V. Fokin and K. B. Sharpless, *Angew. Chem., Int. Ed.*, 2002, **41**, 2596.
22 V. Hong, S. I. Presolski, C. Ma and M. G. Finn, *Angew. Chem., Int. Ed.*, 2009, **48**, 9879.
23 A. V. Ustinov, I. A. Stepanova, V. V. Dubnyakova, T. S. Zatsepin, E. V. Nozhevnikova and V. A. Korshun, *Rus. J. Bioorg. Chem.*, 2010, **36**, 401, and references therein.
24 A. H. El-Sagheer and T. Brown, *Chem. Soc. Rev.*, 2010, **39**, 1388, and references therein.
25 K. Gogoi, M. V. Mane, S. S. Kunte and V. A. Kumar, *Nucleic Acids Res.*, 2007, **35**, e139.
26 A. A. Koshkin, S. K. Singh, P. Nielsen, V. K. Rajwanshi, R. Kumar, M. Meldgaard, C. E. Olsen and J. Wengel, *Tetrahedron*, 1998, **54**, 3607; S. Obika, D. Nanbu, Y. Hari, J. Andoh, K. Morio, T. Doi and T. Imanishi, *Tetrahedron Lett.*, 1998, **39**, 5401.
27 S. K. Singh, R. Kumar and J. Wengel, *J. Org. Chem.*, 1998, **63**, 6078.
28 M. D. Sørensen, L. Kvaernø, T. Bryld, A. E. Håkansson, L. Keinicke, B. Verbeure, P. Herdewijn and J. Wengel, *Nucleic Acids Res. Suppl.*, 2001, **1**, 25.
29 P. J. Hrdlicka;, B. R. Babu, M. D. Sørensen, N. Harrit and J. Wengel, *J. Am. Chem. Soc.*, 2005, **127**, 13293; M. Kalek, A. S. Madsen and J. Wengel, *J. Am. Chem. Soc.*, 2007, **129**, 9392; I. V. Astakhova, V. A. Korshun, K. Jahn, J. Kjems and J. Wengel, *Bioconjugate Chem.*, 2008, **19**, 1995.
30 Y. Gao, X.-L. Liu and X. R. Li, *Int. J. Nanomed.*, 2011, **6**, 1017, and references therein; F. J. Hernandez, N. Kalra, J. Wengel and B. Vester, *Bioorg. Med. Chem. Lett.*, 2009, **19**, 6585; M. Terrazas and E. T. Kool, *Nucleic Acids Res.*, 2009, **37**, 346.
31 K. K. Karlsen and J. Wengel, *Nucleic Acid Ther.*, 2012, **22**, 366, and references therein.
32 M. W. Johannsen, L. Crispino, M. C. Wamberg, N. Kalra and J. Wengel, *Org. Biomol Chem.*, 2011, **9**, 234.
33 M. Noda and Y. Teranishi, *Nature*, 1982, **297**, 431.
34 E. S. Olson, M. A. Whitney, B. Friedman, T. A. Aguilera, J. L. Crisp, F. M. Baik, T. Jiang, S. M. Baird, S. Tsimikas, R. Tsien and Q. T. Nguyen, *Integr. Biol.*, 2012, **4**, 595.
35 A. P. Johnston, M. M. Kamphuis, G. K. Such, A. M. Scott, E. C. Nice, J. K. Heath and F. Caruso, *ACS Nano*, 2012, **6**, 6667.
36 I. K. Astakhova and J. Wengel, *Chem.–Eur. J.*, 2012, **19**, 1112.
37 A. Søndergaard Jørgensen, P. Gupta, J. Wengel and I. K. Astakhova, *ChemBioChem*, submitted.
38 H. Wu, *et al.*, *Nature*, 2012, **485**, 327.
39 A. A. Thompson, *et al.*, *Nature*, 2012, **485**, 395.
40 S. I. Presolski1, V. P. Hong and M. G. Finn, *Curr. Protoc. Chem. Biol.*, 2011, **3**, 153.
41 Tris[(1-benzyl-1*H*-1,2,3-triazol-4-yl)methyl] amine (TBTA): T. R. Chan, R. Hilgraf, K. B. Sharpless and V. V. Fokin, *Org. Lett.*, 2004, **6**, 2853.
42 M. Manoharan, *Biochim. Biophys. Acta*, 1999, **1**, 117.
43 M. Mandel and J. Marmur, *Methods Enzymol.*, 1968, **12**, 198.
44 W. Saenger, *Principles of Nucleic Acid Structure*, Springer-Verlag, New York, Berlin, Heidelberg, Tokyo, 1983; F. Yuan, L. Griffin, L. Phelps, V. Buschmann, K. Weston and N. L. Greenbaum, *Nucleic Acids Res.*, 2007, **35**, 2833.
45 J. Wengel, B. Vester, L. B. Lundberg, S. Douthwaite, M. D. Sørensen, B. R. Babu, M. J. Gait, A. Arzumanov, M. Petersen and J. T. Nielsen, *Nucleosides, Nucleotides Nucleic Acids*, 2003, **22**, 601.
46 For example, L. Crouzier, C. Dubois, J. Wengel and R. N. Veedu, *Bioorg. Med. Chem. Lett.*, 2012, **22**, 4836.

47 J. Kurreck, E. Wyszko, C. Gillen and V. A. Erdmann, *Nucleic Acids Res.*, 2002, **30**, 1911; N. K. Andersen, H. Døssing, F. Jensen, B. Vester and P. Nielsen, *J. Org. Chem.*, 2011, **76**, 6177.
48 O. S. Gudmundsson, K. Nimkar, S. Gangwar, T. Siahaan and R. T. Borchardt, *Pharm. Res.*, 1999, **16**, 16.
49 *MacroModel, version 9.1, Schrödinger*, LLC, New York, NY, 2005.
50 S. J. Weiner, P. A. Kollman, D. T. Nguen and D. A. Case, *J. Comput. Chem.*, 1986, **7**, 230.
51 S. J. Weiner, P. A. Kollman, D. A. Case, U. C. Singh, C. Ghio, G. Alagona, S. Profeta and P. K. Weiner, *J. Am. Chem. Soc.*, 1984, **106**, 765.
52 U. Burkert and N. L. Allinger, *Molecular Mechanics, ACS Monograph 177*, American Chemical Society, Washington, DC, 1982.
53 J. Orans, E. A. McSweeney, R. R. Iyer, M. A. Hast, H. W. Hellinga, P. Modrich and L. S. Beese, *Cell*, 2011, **145**, 212.
54 A. H. El-Sagheer and T. Brown, *Acc. Chem. Res.*, 2012, **45**, 1258, and references therein.
55 M. J. Gait, *Cell. Mol. Life Sci.*, 2003, **60**, 1.
56 D. J. Lee, S. H. Yang, G. M. Williams and M. A. Brimble, *J. Org. Chem.*, 2012, **77**, 7564; G. Pourceau, A. Meyer, J.-J. Vasseur and F. Morvan, *J. Org. Chem.*, 2009, **74**, 1218.
57 A. Salic and T. J. Mitchison, *Proc. Natl. Acad. Sci. U. S. A.*, 2008, **105**, 2415.